

Hydrogel Microspheres by Thermally Induced Coacervation of Poly(*N,N*-dimethylacrylamide-*co*-glycidyl methacrylate) Aqueous Solutions

Xiangchun Yin and Harald D. H. Stöver*

Department of Chemistry, McMaster University, Hamilton, Ontario, Canada L8S 4M1

Received June 13, 2003; Revised Manuscript Received October 17, 2003

ABSTRACT: Aqueous solutions of poly(*N,N*-dimethylacrylamide-*co*-glycidyl methacrylate) (DMA–GMA) are shown to undergo liquid–liquid phase separation upon heating. The phase transition temperatures as measured by the cloud point method decreased with increasing levels of the hydrophobic GMA comonomer. The initially formed coacervate microdroplets could be cross-linked by addition of polyamines. The morphology of the resulting hydrogel microspheres depends on both coacervation conditions and cross-linking conditions. Specifically, colloidal stable microspheres were formed at temperatures slightly above the phase transition temperatures, while agglomeration took place at higher temperatures. Low molecular weight polyamines are effective internal cross-linkers for the coacervate droplets, while higher molecular weight polyamines resulted in agglomeration. Addition of sodium dodecyl sulfate increased the phase transition temperatures of polymer solutions dramatically, while addition of poly(vinylpyrrolidone) (PVP) did not affect the phase separation temperatures and could be used as a steric stabilizer.

Introduction

Polymer systems that show phase transitions in response to environmental stimuli have potential uses in biotechnology, chemical separation, and catalysis.¹ Thermally induced phase separations of aqueous polymer solutions are attractive as they require no additives and are usually reversible. Poly(*N*-isopropylacrylamide) (pNIPAM) undergoes a sharp coil–globule transition at its lower critical solution temperature (LCST) of around 32 °C and precipitates in form of a solid driven by both hydrophobic interactions between its isopropyl groups and hydrogen bonding between the amide groups.^{2–7} Aqueous solutions of poly(*N,N*-dimethylacrylamide) (pDMA), having only two methyl groups and no hydrogen-bonding ability, do not show LCST's below 100 °C. DMA copolymers with hydrophobic comonomers do exhibit LCST behavior, though unlike pNIPAM solutions, they undergo liquid–liquid phase separations.^{8–10} Recently, Akashi's group described similar liquid–liquid phase separations of linear and cross-linked copolymers comprised of *N*-vinylformamide or *N*-vinylacetamide and vinyl acetate as respectively the hydrophilic and hydrophobic components.¹¹ In both cases the phase transition temperature depends on the comonomer ratio. Similar phase separations are known in certain proteins such as elastin and are being explored for uses in protein separation and tissue engineering.^{12,13}

Such liquid–liquid phase separations of aqueous polymer solutions into a polymer-rich coacervate phase and a polymer-lean equilibrium phase are collectively called coacervation^{14–16} and are generally divided into two classes: complex coacervation and simple coacervation. Complex coacervation involves polyelectrolyte complexation, while simple coacervation is caused by changing the solvent composition or the solution temperature. Both processes have been used for protein separation and for preparing hydrogel microparticles.^{17–20} Natural polymers such as gelatin/acacia and chitosan/

alginate still form the majority of materials used to make microparticles via complex coacervation.^{21–23} A few studies have been carried out using synthetic polymers.^{24–27}

Recently, our group prepared hydrogel microspheres by a novel two-step process of complex coacervation followed by cross-linking, using reactive polyanions and polyamines, and investigated the thermoresponsive properties of these copolymers.^{27,28} Independently, Tirelli's group developed a similar concept based on Michael-addition self-cross-linking of a mixture of thiolate and acrylate-functional pluronic polymers, both below and above their LCST.²⁹

In this paper, we report the thermally induced coacervation of aqueous solutions of poly(*N,N*-dimethylacrylamide-*co*-glycidyl methacrylate) copolymers and the covalent cross-linking of the resulting coacervate droplets in a second step with polyamines to form hydrogel microspheres. While presently carried out using small polyamines, and aimed at forming microspheres, these processes may also be carried out using chitosan or other biocompatible polyamines and hence lead to new self-cross-linking materials useful in a variety of applications including cell encapsulations and biomaterial design.

Experimental Section

Materials. *N,N*-Dimethylacrylamide (DMA), glycidyl methacrylate (GMA), *N*-isopropylacrylamide (NIPAM), sodium dodecyl sulfate (SDS), poly(vinylpyrrolidone) (PVP) (M_w , 40 000), ethylenediamine (EDA), tetraethylenepentamine (TEPA), and polyethylenimine (PEI) of different molecular weights were purchased from Aldrich and used as received. 2,2'-Azobis(isobutyronitrile) (AIBN) was obtained from American Polymer Standards Laboratories and recrystallized from methanol. Tetrahydrofuran (THF) and anhydrous diethyl ether were obtained from Caledon Laboratories. THF was refluxed over sodium and distilled prior to use.

Preparation of Poly(*N,N*-dimethylacrylamide-*co*-glycidyl methacrylate) (DMA–GMA) Copolymers. For a typical procedure, 6.57 g of *N,N*-dimethylacrylamide (0.066 mol) and 2.82 g of 95 wt % glycidyl methacrylate (0.019 mol)

* Corresponding author: e-mail stoverh@mcmaster.ca.

were dissolved in 100 mL of THF in a 125 mL HDPE plastic screw cap bottle. Oxygen was removed by bubbling nitrogen through the mixture before adding 0.070 g of AIBN (4.26×10^{-4} mol, 0.5 mol % relative to monomers). Polymerization was carried out at 70 °C for 1 h by rolling the bottles in a thermostated reactor fitted with a set of horizontal rollers. The product was precipitated into 500 mL of diethyl ether and dried under vacuum at 40 °C to provide 3.0 g of polymer (yield 32%).

Molecular weights of copolymers were determined using a gel permeation chromatograph consisting of a Waters 515 HPLC pump, three Ultrastaygel columns (500–20K, 500–30K, 5K–600K Da), and a Waters 2414 refractive index detector, using THF as solvent at a flow rate of 1 mL min⁻¹ and narrow disperse polystyrene as calibration standards.

¹H NMR spectra of the copolymers were recorded on a Bruker AC 200 using chloroform-*d* as the solvent. Compositions of DMA–GMA copolymers were determined by integration of characteristic peaks.

Measurement of Phase Transition Temperatures. Phase transition temperatures of aqueous solutions of DMA–GMA copolymers were measured using the cloud point method. An automatic PC-Titrator (Mandel) equipped with a temperature probe and with a photometer incorporating a 1 cm path length fiber-optics probe (GT-6LD, Mitsubishi) was used to trace the phase transition by monitoring the transmittance of a beam of white light. The turbidity of the solution was recorded as photoinduced voltage (millivolts). The phase transition temperature was defined as the inflection point of the mV vs temperature curve, as determined by the maximum in the first derivative. The heating rate was 1.0 °C min⁻¹, and concentrations of polymer solutions were 0.2, 0.5, 1.0, and 2.0 wt %.

Preparation of Hydrogel Microspheres. The DMA–GMA copolymers were dissolved in deionized water at a temperature below the phase transition temperature. The solutions were stirred and heated above the phase separation temperature to induce coacervation. After phase equilibration, polyamine was added to cross-link the formed coacervate droplets.

In a typical reaction, 30 g of a 0.5 wt % DMA–GMA43 solution was stirred at 1000 rpm and heated to 40 °C in a 50 mL jacketed beaker. After the coacervate was equilibrated at 40 °C for 5 min, 1.5 mL of 2.0 wt % ethylenediamine was added. The cross-linking reaction was allowed to proceed for 2 h, and the resulting microspheres were separated by centrifugation at 3000 rpm for 10 min. The microspheres were washed with deionized water to remove unreacted materials and dried in a vacuum at 65 °C to provide 0.03 g of microspheres (yield 16.7%).

Characterization of Hydrogel Microspheres. Optical images of the microspheres were recorded at room temperature using an Olympus BH-2 microscope equipped with a Kodak DC 120 Zoom digital camera.

Morphologies of the microspheres were examined using a Phillips ElectroScan 2020 environmental scanning electron microscope (ESEM). ESEM samples were prepared by depositing a drop of aqueous microsphere suspension onto a glass-covered ESEM stub, drying under vacuum, and sputter-coating with about 5 nm of gold.

Results and Discussion

Synthesis and Properties of DMA–GMA Copolymers. Copolymerization with glycidyl methacrylate (GMA) permits both thermal coacervation and subsequent cross-linking of the resulting coacervate droplets to form hydrogel microspheres. The copolymerization conversions were kept below 30% in order to limit copolymer composition drifts.

¹H NMR spectra of DMA and GMA homopolymers and of a copolymer are shown in Figure 1, with peak assignments from the literature.^{30,31} Copolymer compositions (Table 1) were estimated by comparing the peak area (A) of a GMA methyleneoxy protons (f) at 4.27 ppm, with the total peak area (B) between 2.3 and 3.3 ppm,

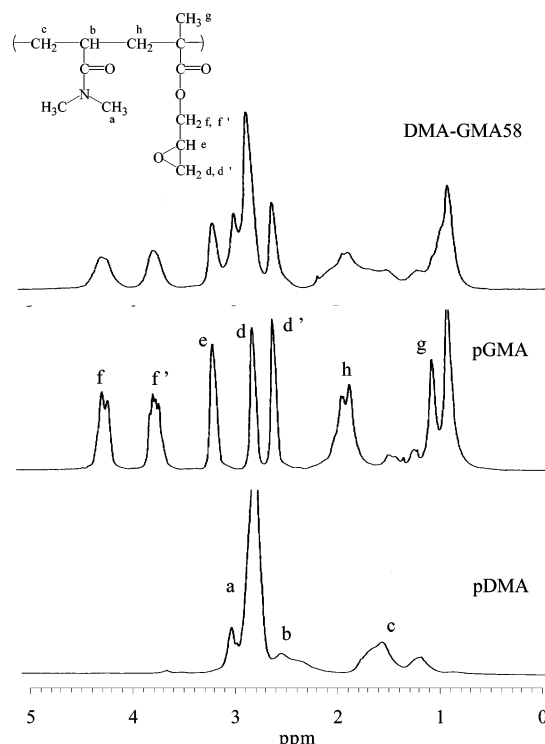


Figure 1. ¹H NMR spectra of pDMA and pGMA homopolymers and copolymer DMA–GMA58 in chloroform-*d*.

Table 1. Compositions and Phase Transition Temperatures of Poly(*N,N*-dimethylacrylamide-*co*-glycidyl methacrylate) (DMA–GMA) Copolymers

DMA–GMA copolymer	GMA amount (mol %)		M_n^b	M_w/M_n^b	T_p^c (°C)
	in feed	in polymer ^a			
DMA–GMA12	10.0	12.2	7.3×10^3	1.6	none ^d
DMA–GMA19	16.6	19.4	7.0×10^3	1.6	none ^d
DMA–GMA32	22.2	32.2	6.4×10^3	1.8	58.7
DMA–GMA36	26.3	35.6	7.0×10^3	1.8	35.4
DMA–GMA43	28.6	42.9	7.8×10^3	1.9	27.6
DMA–GMA47	33.3	46.5	8.6×10^3	1.9	7.6
DMA–GMA58	40.0	57.7	1.4×10^4	1.7	not water-soluble ^e

^a Estimated by ¹H NMR. ^b Determined by GPC. ^c Inflection points of the cloud point curves measured at 0.5 wt % polymer concentration. ^d Below 100 °C. ^e Even at 0 °C.

which includes seven protons (a, b) from DMA and three protons (e, d, d') from GMA. The mole ratio of DMA to GMA in each copolymer is then found as (B–3A)/7A.

The temperature-dependent phase separation of aqueous solutions of different DMA–GMA copolymers was investigated by turbidimetry. Figure 2 shows photovoltage vs temperature curves for four DMA–GMA compositions and for poly(NIPAM), with zero volt corresponding to an opaque solution. The compositions and their corresponding phase transition temperatures (T_p) are shown in Table 1.

The pNIPAM solution shows the characteristically sharp liquid–solid phase transition at about 32 °C, with the complete opacity above the LCST due to scattering from the desolvated pNIPAM particles.

Aqueous solutions of DMA–GMA copolymers with less than 20 mol % GMA do not show thermal phase transitions (Table 1). GMA contents between 30 and 45% result in liquid–liquid phase transition, indicating

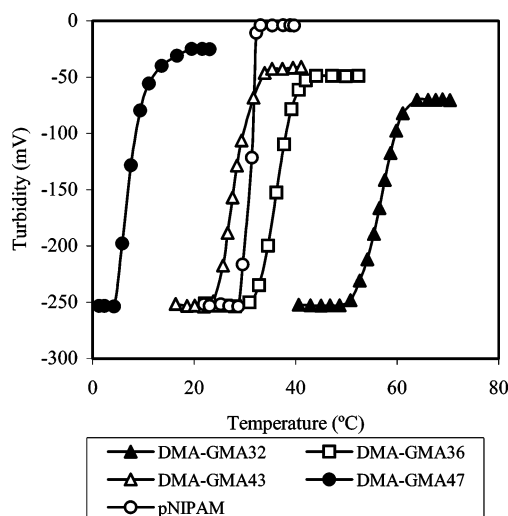


Figure 2. Photovoltaic cloud point curves for 0.5 wt % aqueous solutions of DMA-GMA and pNIPAM, with -250 mV corresponding to a transparent solution.

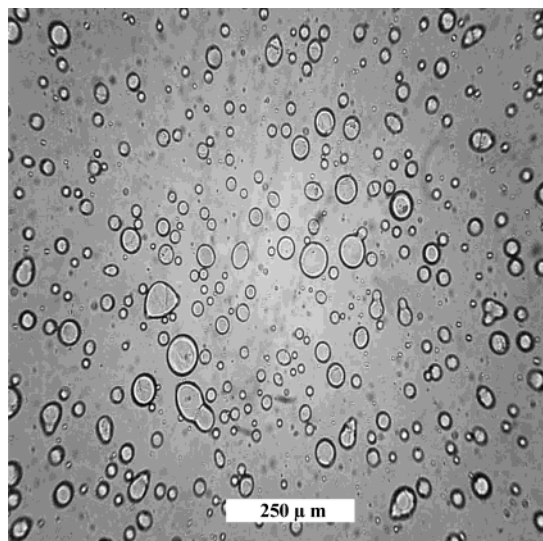


Figure 3. Optical microscope image of coacervate droplets in 1 wt % aqueous DMA-GMA47 solution at room temperature (25 °C).

both the finite transmittance above their cloud points (Figure 2) and the separation into a viscous polymer-rich bottom layer and a transparent polymer-poor top layer upon standing. DMA-GMA copolymers with more than 50% GMA are not soluble in water, even at 0 °C.

Figure 3 presents an optical microscope image of a 1.0 wt % DMA-GMA47 solution at room temperature, showing the expected liquid coacervate droplets.

The phase separation temperatures of these copolymer solutions drop by several degrees as the polymer concentration is increased from 0.2 to 2% (Figure 4). It is currently not clear whether this behavior is due to a true shift of the liquid-liquid phase separation temperature with concentration or an artifact of the cloud point measurement method, where droplet size and refractive index difference may affect the turbidity. Similar concentration dependencies have been reported for the liquid-solid phase transition of poly(*N,N*-diethylacrylamide) and were attributed to the cloud point method.³² The phase transition behavior of aqueous solutions of DMA copolymers will be studied by microcalorimetry and light scattering in future studies.

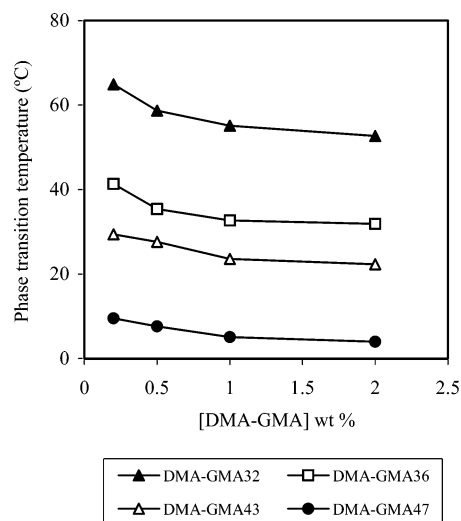


Figure 4. Effects of polymer concentration on the phase separation temperatures of DMA-GMA solutions as measured by the cloud point method.

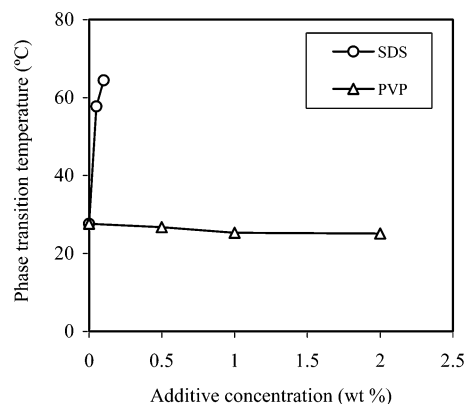


Figure 5. Effects of additives on phase separation temperatures of 0.5 wt % DMA-GMA43 solutions.

Phase transition temperatures of thermally responsive polymer solutions commonly increase with the addition of surfactants up to the critical aggregation concentration, through formation of hydrophilic polymer-surfactant complexes.^{33,34} Figure 5 shows that adding 0.1 wt % SDS (ca. 3.5 mM) sodium dodecyl sulfate (SDS) increases the phase transition temperature of a 0.5 wt % DMA-GMA43 solution by about 37 °C by introducing charges to the copolymer.

In contrast, adding poly(vinylpyrrolidone) (PVP) does not significantly affect the phase transition temperatures (Figure 5), indicating that PVP does not bind to DMA-GMA copolymers in aqueous solutions, a result similar to that known for pNIPAM.³⁵

Cross-Linking of DMA-GMA Coacervate Droplets. Coacervate microdroplets are inherently unstable and will coalesce into a bulk coacervate phase in the absence of a dispersing force. However, they may be cross-linked to form colloidal stable hydrogel microspheres. The thermally induced DMA-GMA coacervate droplets described here were designed to be cross-linked by addition of diamines and polyamines to the aqueous phase after phase separation.

Figure 6 shows the environmental scanning electron microscopy (ESEM) images of cross-linked hydrogel microspheres prepared by addition of ethylenediamine to DMA-GMA coacervate droplets. Coacervation and cross-linking were carried out at temperatures slightly

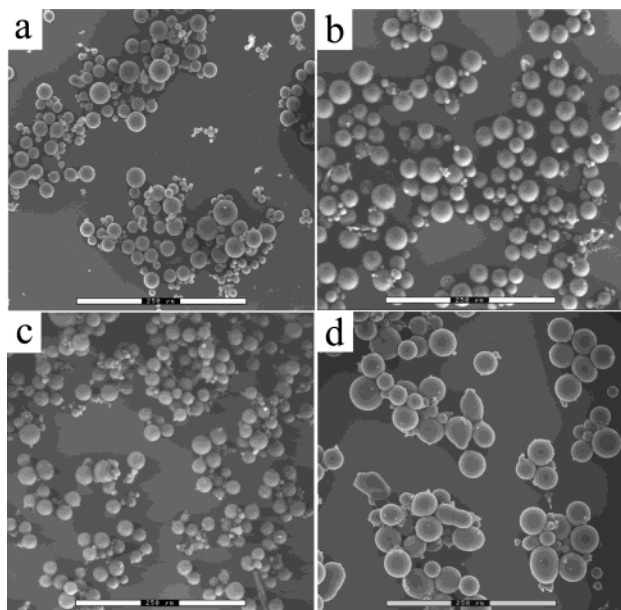


Figure 6. ESEM images of hydrogel microspheres prepared by cross-linking thermally induced coacervates (30 mL, 0.5 wt %) with ethylenediamine (1.5 mL, 2.0 wt %). (a) DMA-GMA32 at 60 °C, (b) DMA-GMA36 at 40 °C, (c) DMA-GMA43 at 30 °C, (d) DMA-GMA47 at 20 °C. Scale bars are 250 μm .

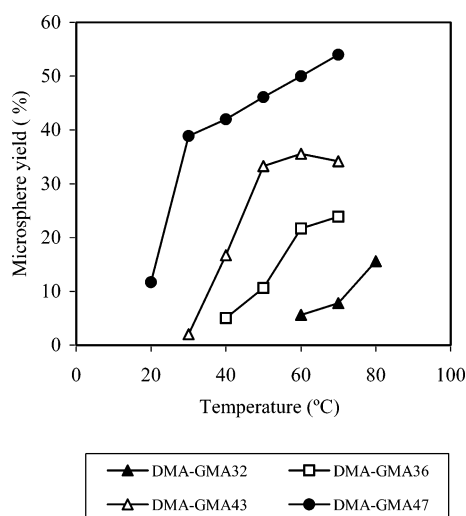


Figure 7. Yields of microspheres obtained by cross-linking at different temperatures.

above the corresponding phase transition temperatures. Under these conditions, ethylenediamine diffuses into the coacervates and reacts with epoxy groups in the polymer chain. Cross-linking is promoted over simple functionalization by the enrichment of the polymer in the coacervate phase, and no cross-linking or gelation is observed when ethylenediamine is added at temperatures below the phase transition temperature.

The cross-linked microspheres are stable during workup. The conversion of epoxy groups to hydroxyl groups and the incorporation of amines renders the microspheres more hydrophilic and even ionic and removes their temperature-responsive properties.

Coacervate and Microsphere Yield. Figure 7 shows the yield of cross-linked microspheres as a function of cross-linking temperatures. The microsphere yields, which reflects both the coacervate yield and the cross-linking efficiency, increase with increasing cross-linking temperatures.

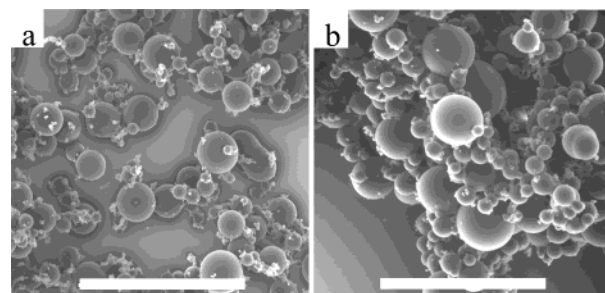


Figure 8. ESEM images of hydrogel microspheres prepared by cross-linking DMA-GMA43 coacervates with ethylenediamine at (a) 40 and (b) 70 °C. Scale bars are 250 μm .

The phase transition of DMA-GMA47 aqueous solution occurs below room temperature, which allows us to easily measure the coacervate yield itself. The coacervate yield of a 0.5 wt % DMA-GMA47 aqueous solution at 25 °C is 26%, which roughly corresponds to the microsphere yield in that temperature range (Figure 7). This indicates that the microsphere yield mainly depends on the coacervation process and that cross-linking of the formed coacervate is quite efficient. Hence, the coacervation yield can be estimated through the microsphere yield.

This temperature-dependent coacervation yield is partly due to the compositional distribution of the copolymer. *N,N*-Dimethylacrylamide and glycidyl methacrylate monomers have different reactivity ratios, and chains generated at the beginning of the polymerization should contain more GMA, be more hydrophobic, and have lower cloud point temperatures than chains generated later in the polymerization. The resulting compositional distribution will broaden the temperature range over which coacervation occurs, even though we limited our polymerizations to about 30% monomer conversion. In the future we will explore living/controlled radical copolymerizations to further narrow the compositional distributions of the copolymers.

As well, the liquid-liquid phase separations are continuous processes, in contrast to pNIPAM's liquid-solid precipitation. The consequences of this progressive chain collapse will be explored in future work.

Microsphere Morphology. Figure 8 presents ESEM micrographs of microspheres prepared from 0.5 wt % DMA-GMA43 at 40 and 70 °C. Compared to the microspheres cross-linked at 30 °C shown in Figure 6c, cross-linking at these higher temperatures leads to more and larger microspheres, but with less colloidal stability. This is expected, given the same dispersing force but a higher yield of more viscous and more hydrophobic coacervates. In addition, the more efficient cross-linking at higher temperature may cause more interparticle bonds that would contribute to the observed aggregation.

Figure 9 presents the effect of polyamine size on the morphologies of cross-linked coacervate microspheres. Colloidally stable microspheres are obtained upon cross-linking with the small amines such as ethylenediamine or tetraethylenepentamine (Figure 9a). Using linear PEI 432 leads to more aggregation, and branched PEI 1800 gives microspheres that appear more fused, plausibly due to enhanced bridging between microspheres.

Increasing the polymer concentration increases both the amount of coacervate dispersed in the continuous medium and the viscosity. In turn, this leads to larger

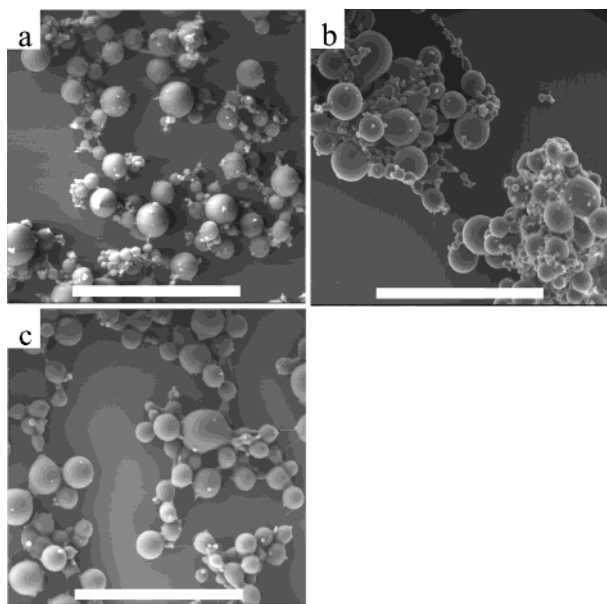


Figure 9. ESEM images of hydrogel microspheres prepared by cross-linking DMA-GMA43 coacervates at 40 °C with (a) TEPA, (b) linear PEI 423, and (c) branched PEI 1800. Scale bars are 250 μm .

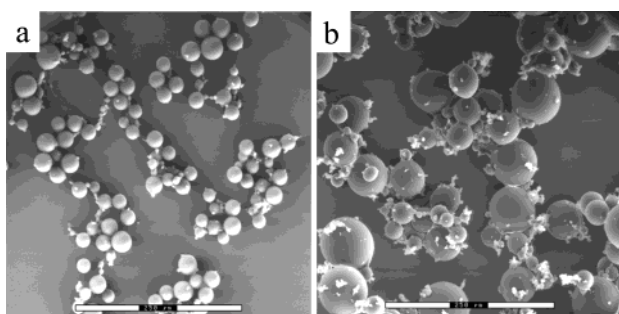


Figure 10. ESEM images of hydrogel microspheres prepared at 40 °C from 30 mL of (a) 0.2 wt % and (b) 2.0 wt % DMA-GMA43 solutions and ethylenediamine. Amine-to-polymer ratios were held constant corresponding to 1.5 mL of 2% amine solution for (b). Scale bars are 250 μm .

particle sizes and broader size distributions (Figure 10a,b).

Effect of Adding PVP. As discussed above, PVP has no significant effect on the phase transition temperature of DMA-GMA solutions and hence apparently does not bind to the copolymer below its cloud point. However, PVP may bind to the more hydrophobic coacervate and hence may provide some steric stabilization to the droplets and to the cross-linked microspheres. Figure 11 shows that addition of 1 wt % PVP reduces the particle size and the degree of aggregation compared to Figure 8a.

Conclusion

Poly(*N,N*-dimethacrylamide-*co*-glycidyl methacrylate) (DMA-GMA) copolymers have been prepared by free radical copolymerizations. The thermal phase separation of DMA-GMA aqueous solutions is a coacervation process, and the phase transition temperature decreases with increasing GMA content.

The DMA-GMA coacervate droplets can be cross-linked by adding diamines and small polyamines. The yield, size, and size distribution of the resulting hydrogel microspheres increase with increasing reaction temper-

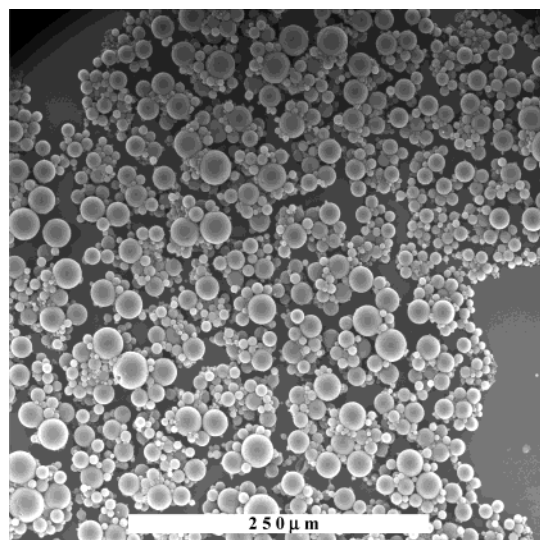


Figure 11. ESEM images of hydrogel microspheres prepared from DMA-GMA43 coacervates in the presence of 1 wt % PVP at 40 °C.

ature and polymer concentration. The size and aggregation of the microspheres can be reduced by addition of PVP.

Acknowledgment. We thank Dr. Nicholas Burke for valuable discussions and the Natural Sciences and Engineering Research Council of Canada and 3M Canada Co. for financial support.

References and Notes

- (1) Pelton, R. *Adv. Colloid Interface Sci.* **2000**, *85*, 1–33.
- (2) Zhu, P. W.; Napper, D. H. *J. Colloid Interface Sci.* **1994**, *168*, 380–385.
- (3) Wu, C.; Zhou, S. *Macromolecules* **1995**, *28*, 8381–8387.
- (4) Zhu, P. W.; Napper, D. H. *Langmuir* **1996**, *12*, 5992–5998.
- (5) Qiu, X.; Wu, C. *Macromolecules* **1997**, *30*, 7921–7926.
- (6) Maeda, Y.; Higuchi, T.; Ikeda, I. *Langmuir* **2000**, *16*, 7503–7509.
- (7) Maeda, Y.; Nakamura, T.; Ikeda, I. *Macromolecules* **2001**, *34*, 1391–1399.
- (8) Mueller, K. F. *Polymer* **1992**, *33*, 3470–3476.
- (9) Miyazaki, H.; Kataoka, K. *Polymer* **1996**, *37*, 681–685.
- (10) Shibamura, T.; Aoki, T.; Sanui, K.; Ogata, N.; Kikuchi, A.; Sakurai, Y.; Okano, T. *Macromolecules* **2000**, *33*, 444–450.
- (11) Yamamoto, K.; Serizawa, T.; Akashi, M. *Macromol. Chem. Phys.* **2003**, *204*, 1027–1033.
- (12) Yang, G.; Woodhouse, K. A.; Yip, C. M. *J. Am. Chem. Soc.* **2002**, *124*, 10648–10649.
- (13) Betre, H.; Setton, L. A.; Meyer, D. E.; Chilkoti, A. *Biomacromolecules* **2002**, *3*, 910–916.
- (14) Burgess, D. J. *J. Colloid Interface Sci.* **1990**, *140*, 227–238.
- (15) Menger, F. M.; Sykes, B. M. *Langmuir* **1998**, *14*, 4131–4137.
- (16) Menger, F. M.; Peresypkin, A. V.; Caran, K. L.; Apkarian, R. P. *Langmuir* **2000**, *16*, 9113–9116.
- (17) Arshady, R. *Polym. Eng. Sci.* **1990**, *30*, 905–914.
- (18) Prokop, A.; Hunkeler, D.; DiMari, S.; Haralson, M.; Wang, T. G. *Adv. Polym. Sci.* **1998**, *136*, 1–51.
- (19) Wen, Y.; Dubin, P. L. *Macromolecules* **1997**, *30*, 7856–7861.
- (20) Kaibara, K.; Okazaki, T.; Bohidar, H. B.; Dubin, P. L. *Biomacromolecules* **2000**, *1*, 100–107.
- (21) Burgess, D. J.; Singh, O. N. *J. Pharm. Pharmacol.* **1993**, *45*, 586–591.
- (22) Chandy, T.; Mooradian, D. L.; Rao, G. H. *J. Appl. Polym. Sci.* **1998**, *70*, 2143–2153.
- (23) Tiyaboonchai, W.; Woiszwillo, J.; Middaugh, C. R. *J. Pharm. Sci.* **2001**, *90*, 902–914.
- (24) Cohen, S.; Baño, M. C.; Visscher, K. B.; Chow, M.; Allcock, H. R.; Langer, R. *J. Am. Chem. Soc.* **1990**, *112*, 7832–7833.
- (25) Wen, S.; Yin, X.; Stevenson, W. T. K. *Biomaterials* **1991**, *12*, 374–384.
- (26) Andrianov, A. K.; Chen, J.; Payne, L. G. *Biomaterials* **1998**, *19*, 109–115.

- (27) Yin, X.; Stöver, H. D. H. *Macromolecules*, in press.
- (28) Yin, X.; Stöver, H. D. H. *Macromolecules* **2002**, *35*, 10178–10181.
- (29) Cellesi, F.; Tirelli, N.; Hubbell, J. A. *Macromol. Phys. Chem.* **2002**, *203*, 1466–1472.
- (30) Miron, Y.; Morawetz, H. *Macromolecules* **1969**, *2*, 162–165.
- (31) Virtanen, J.; Tenhu, H. *J. Polym. Sci., Part A: Polym. Chem.* **2001**, *39*, 3716–3725.
- (32) Idziak, I.; Avoce, D.; Lessard, D.; Gravel, D.; Zhu, X. X. *Macromolecules* **1999**, *32*, 1260–1263.
- (33) Schild, H. G.; Tirrell, D. A. *Langmuir* **1991**, *7*, 665–671.
- (34) Lee, L.; Cabane, B. *Macromolecules* **1997**, *30*, 6559–6566.
- (35) Subotic, D. V.; Wu, X. Y. *Ind. Eng. Chem. Res.* **1997**, *36*, 1303–1309.

MA034809I